

Title no. 84-M35

Effect of Cracking on Drying Permeability and Diffusivity of Concrete



by Zdeněk P. Bažant, Siddik Şener, and Jin-Keun Kim

The increase of overall drying permeability and diffusivity of concrete due to cracking is determined experimentally and formulated mathematically. The test specimens are C-shaped beams deformed by a tie rod and reinforced on the tensile face so that uniformly spaced cracks are produced. The difference in the loss of weight for various drying periods between cracked and uncracked specimens is measured and used to quantify the effect on permeability and diffusivity. The overall drying diffusivity and permeability in the cracking direction, which is theoretically proportional to the crack width cubed and inversely proportional to the crack spacing, is found to increase about 2.25 times for crack width 0.1 mm and crack spacing 70 mm. Although appreciable, this value is two orders of magnitude less than the theoretical upper bound predicted on the basis of viscous flow calculation if it is assumed that the cracks are of constant thickness, have planar walls, and are continuous. It is concluded that even though the major cracks are seen to be continuous on the specimen surface, they must be discontinuous in the specimen interior, perhaps being interconnected by much narrower necks with a width about 10 times smaller. This fact is of interest for deducing fracture process zone models from visual observations of cracks on the specimen surface. Although approximate, the presently derived formula for the increase of diffusivity and permeability is directly usable in finite element programs for drying or wetting of concrete.

Keywords: concretes; cracking (fracturing); crack width and spacing; diffusivity; drying; measurement; moisture; permeability.

Calculations of shrinkage, creep, and other mechanical behavior of concrete necessitate a realistic prediction of the profiles of pore humidity or specific water content throughout a concrete structure at various times. Such calculations are now frequently conducted in various advanced finite element codes for concrete structures.¹ However, in the present practice, the permeability and diffusivity values are based on the existing data for intact concrete,¹⁻⁴ and the effect of cracking due to load is neglected. The advantage of this is that the water diffusion problem may be presumably uncoupled from the deformation and cracking problem. It has been acknowledged that this is a simplification, and in fact, a theoretical formula giving an upper

bound for the effect of concrete cracking on its permeability and diffusivity was derived by Bažant and Raftshol⁵ based on the assumption of viscous laminar flow through continuous planar cracks of constant thickness. No test data appear to exist in the literature to check this formula. To fill this gap, an experimental study has been undertaken at Northwestern University. A brief preliminary report was given at a recent RILEM symposium in Evanston, Ill.,⁶ and the results are reported here in detail.

SPECIMENS AND TEST PROCEDURE

The easiest way to get information on permeability and diffusivity of concrete is to measure the weight loss of a specimen exposed to a controlled drying environment. To determine the overall effect of cracks, which serve as conduits for water vapor and thus enhance moisture transmission, it is necessary to compare specimens that are cracked and uncracked but are otherwise as similar as possible. In choosing the type of specimen, one needs a configuration in which many uniformly spaced cracks can be produced easily at the beginning of the test and the crack width can be kept approximately constant for a long period of drying. These requirements have been met by the C-shaped specimen shown in Fig. 1 and 2.

This shape permits deforming the specimen easily by tightening a steel tie rod (a round bar of diameter 0.5 in. or 12.7 mm). The specimens were cast in the laboratory with a mix ratio cement:sand:gravel:water 1:2:2:0.5 (by weight). The maximum size of the aggregate was $d_a = 0.375$ in. (9.5 mm) and of sand, 0.19 in.

Received Nov. 7, 1986, and reviewed under Institute publication policies. Copyright © 1987, American Concrete Institute. All rights reserved, including the making of copies unless permission is obtained from the copyright proprietors. Pertinent discussion will be published in the July-August 1988 *ACI Materials Journal* if received by Apr. 1, 1988.

Zdeněk P. Bazant, FACI, is a professor at Northwestern University, Evanston, Ill., where he recently served a five-year term as director of the Center for Concrete and Geomaterials. Dr. Bazant is a registered structural engineer and is on the editorial boards of a number of journals. He is Chairman of ACI Committee 446, Fracture Mechanics; a member of ACI Committees 209, Creep and Shrinkage in Concrete; and 348, Structural Safety; and a fellow of ASCE, RILEM, and the American Academy of Mechanics; and Chairman of RILEM's Creep Committee and of SMIRT's Concrete Structures Division.

Siddik Şener is an assistant professor in the Department of Civil Engineering at Istanbul Technical University, Turkey. He obtained his PhD from Istanbul Technical University on the analysis of ribbed cylindrical shells. He has spent the last two years as a visiting scholar at the Center for Concrete and Geomaterials of Northwestern University, conducting both theoretical and experimental research on the inelastic behavior and fracture of concrete and reinforced concrete.

ACI member Jin-Keun Kim is an assistant professor in civil engineering at Korea Advanced Institute of Science and Technology. He obtained his BS and MS degrees from Seoul National University and the PhD from Northwestern University. He is on the editorial board of the Journal of the Architectural Institute of Korea. His research interests include inelastic behavior and fracture of concrete and reinforced concrete structures.

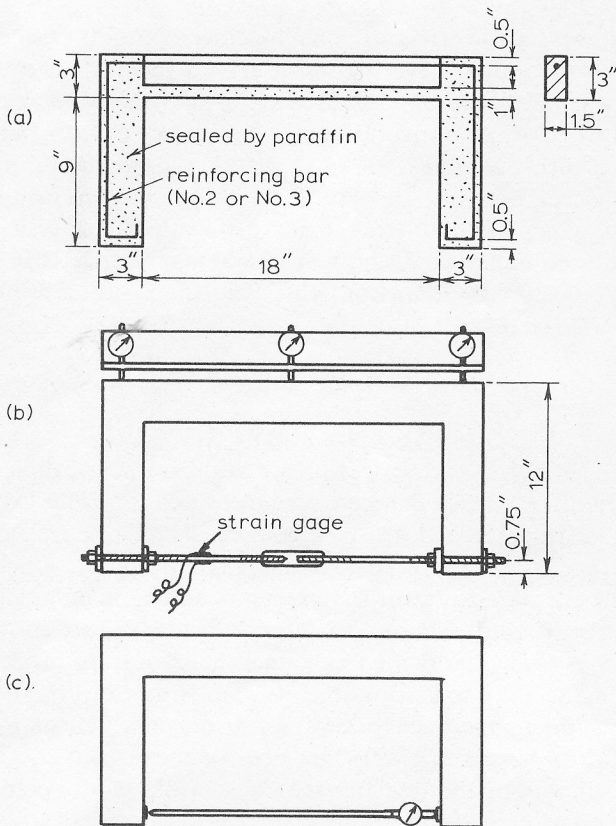


Fig. 1 — C-shaped specimens with crack-producing tie rod

(4.8 mm). The aggregate was crushed dolomitic limestone from the Racine, Wis., quarry, and the sand was a river sand from Antioch, Ill. Ordinary portland cement of ASTM Type I (ASTM C 150) was used. The molds were made of plexiglass (PMMC or polymethylmetacrylate) rather than wood so as to prevent the escape of water. Two sets of specimens were cast: an initial set of two specimens with No. 3 bars (diameter $\frac{3}{8}$ in. or 9.5 mm), and a second set of six specimens with No. 2 bars (diameter $\frac{1}{4}$ in. or 6.4 mm). Each set was

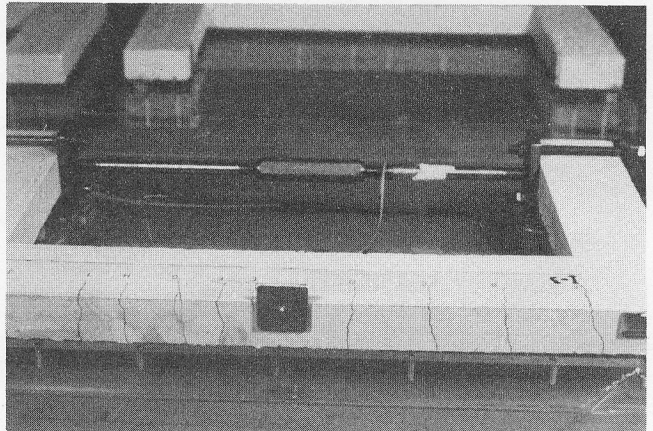
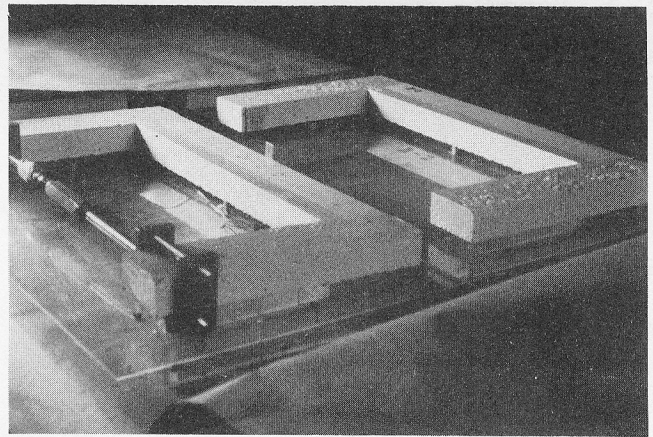


Fig. 2 — Test specimens and cracks produced by drying tie rod

cast from the same batch of concrete. Then each specimen was vibrated, after which it was cured for 24 hours in the mold at a temperature of about 80 F. Then the specimens were demolded and placed in a water bath of 80 F and saturated with lime. The specimens were cured in the bath for six weeks. After that, the specimens were removed from the bath and stored for two weeks at 80 F in a moist room of 98 percent relative humidity. Next, the specimen surfaces were partially sealed with a paraffin coat and then were deformed by means of the tie rod to a prescribed deformation. Drying tests were started in a room of average temperature 76 F and average humidity 50 percent.

The surface area of the specimen that was coated by paraffin is indicated in Fig. 1. The purpose of this coating was to insure that water can escape from the specimen only through the cracked surface and not from the surfaces on which no cracks are produced. Without this partial paraffin coating, the effect of cracking on the drying rate in one part of the specimen would be obfuscated by the drying process in the uncracked parts of the specimen.

The idea behind the method of creating the cracks is to produce them by bending rather than tension since this allows a much simpler and lighter loading device, the tie rod. To make the effect of cracks sufficiently marked, it is necessary to design the specimen so that there are many cracks, and to make evaluation easy, the cracks must be nearly uniformly distributed. If the

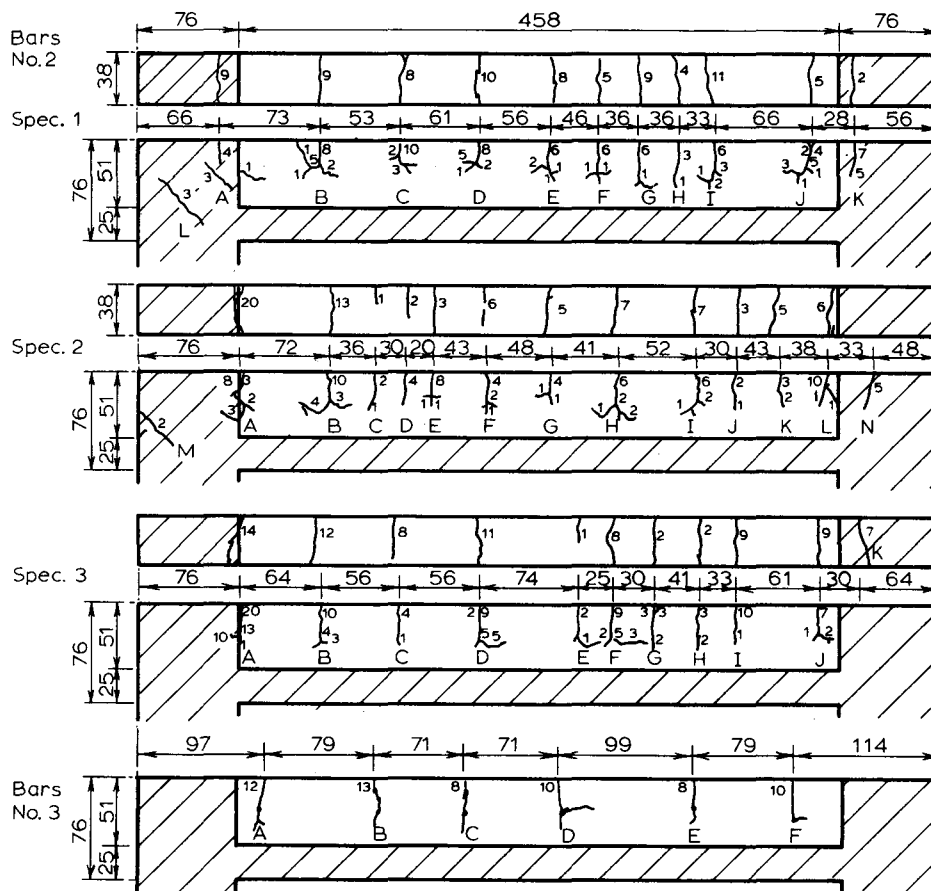


Fig. 3 — Map of crack shapes and crack widths observed by microscope (given in 0.01 mm)

specimen were unreinforced, loading by the tie rod would produce only a single crack. Therefore, the specimen was reinforced. Two sizes of deformed bars were used: No. 2 and No. 3 with diameters 0.25 in. (6.4 mm) and 0.375 in. (9.5 mm), yield strength $f_y = 69,000$ psi, and one bar placed at midthickness with concrete cover 0.5 in. (12.7 mm), as shown in Fig. 1. The reinforcement ratio in the rectangular cross section was 0.011 for No. 2 bars and 0.025 for No. 3 bars. With this reinforcement, it was possible to achieve bending cracks that were distributed quite uniformly (Fig. 3). The major cracks had the average spacing 2.4 in. (60 mm) for No. 2 bars and 3.1 in. (80 mm) for No. 3 bars. The average width of major cracks at the crack mouth was about 0.004 in. (0.10 mm), as measured by an optical microscope (Fig. 3).

The tie rod was initially tensioned to the force 1000 lb (4448 N) for No. 2 bars and 1500 lb (6672 N) for No. 3 bars, as measured by a strain gage on the tie rod. This force produced the desired crack width. Subsequently, the axial force in the bar varied due to creep and shrinkage of the specimen; however, since the tie rod was much stiffer than the bending stiffness of the specimen, the curvature of the drying segment of the specimen and the opening of the cracks remained nearly constant in time, as is desirable for evaluation of the results. The force in the tie rod was measured throughout the test as was the curvature of the drying segment

of the specimen, which was done by measuring deflections by three dial gages. These stress and deformation measurements, however, are not reported and analyzed here since their purpose is to gain understanding of the effect of creep during drying.

For No. 2 bars, the tests included three specimens that were deformed by the tie rod and three identically produced companion specimens that were not deformed. For No. 3 bars, there was only one cracked (drying) and one uncracked (sealed) specimen. The companion specimens were exposed to the same drying environment. The progress of drying for tests for the No. 2 (Fig. 4) bars was monitored by weight measurements on an electronic precision balance whose resolution was 1 g and maximum capacity 24 kg. For the tests with No. 3 bars (Fig. 5), which were carried out first, a less accurate balance was used, and the control of test conditions was poorer. This explains why the scatter of the tests, compared to the hand-drawn smoothing in Fig. 5, is quite large.

Several times during the test, the crack system was observed and mapped with an optical microscope enlarging 100 times.

TEST RESULTS AND THEIR EVALUATION

Fig. 3 shows the maps of the cracks and gives the crack widths (in multiples of 0.01 mm), as measured by microscope. The crack width is seen to be about the

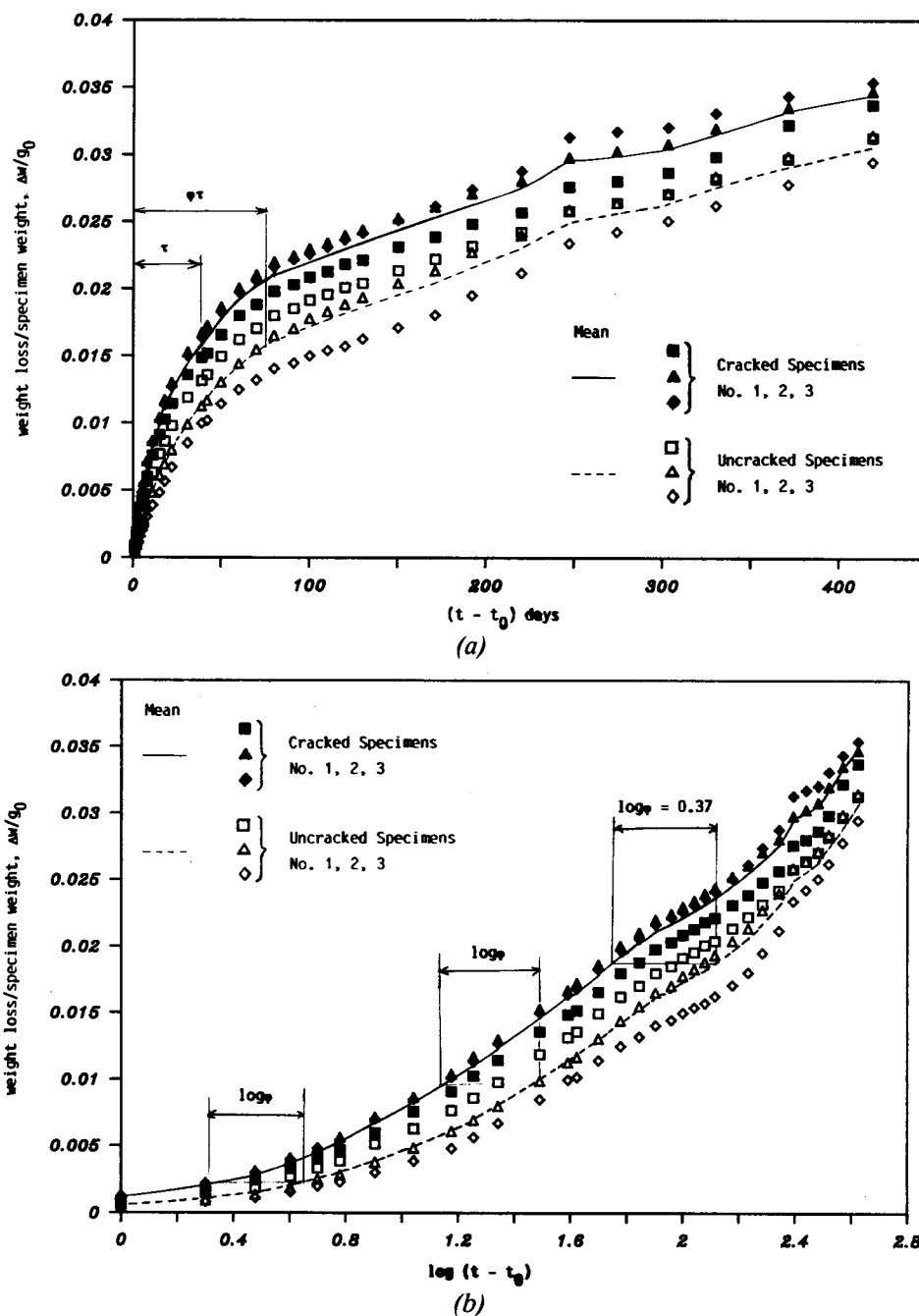


Fig. 4(a) and (b) — Measured relative weight loss of six specimens with No. 2 bars

same for most of the major cracks and for all three deformed specimens. (Only the major cracks matter for the drying rate.)

The evolution of the weight loss for the cracked and uncracked specimens is shown in Fig. 4(a), 4(b), 5(a), and 5(b) by the data points in the actual time and log-time. The solid curve in Fig. 4(a) and 4(b) represents the average values for the three cracked specimens, and the dashed curve represents the average for the three uncracked specimens. Note that despite statistical scatter, each cracked specimen was drying faster than any of the uncracked companion specimens. The difference between the mean weights of the two sets of specimens is significant but not very large.

A noteworthy property of the weight curves in Fig. 4 and 5 is that they initially diverge — the time to reach the same weight being about 2.25 times larger for the

cracked specimens. After this initial period, the weight curves in the actual time are approximately parallel with a constant time lag for the same weight loss, which means that the ratio of the corresponding time between the cracked and uncracked specimens is decreasing. This behavior may be explained by the fact that in the second drying period (after about 130 days for Fig. 4), the relative humidity within the cracks is probably almost in equilibrium with the environment, and the drying process consists predominantly of water migration from the uncracked concrete between the cracks into the cracks themselves. In this drying regime it is obvious that the cracks should contribute little, which explains why the difference between the two weight curves remains constant in the second period. By contrast, in the initial period water migrates towards the drying face both through the cracks and through the

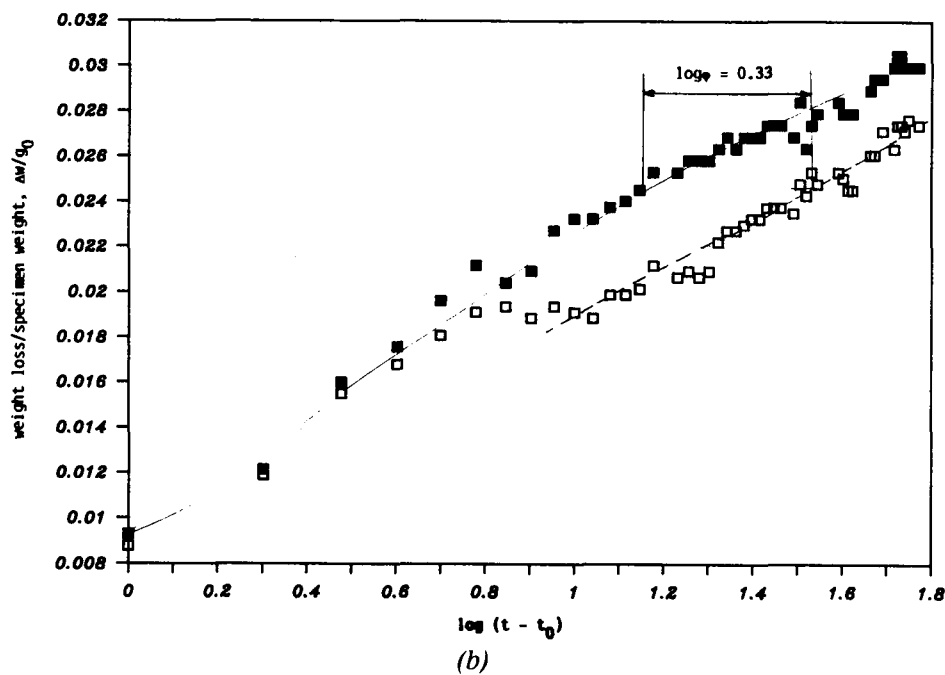
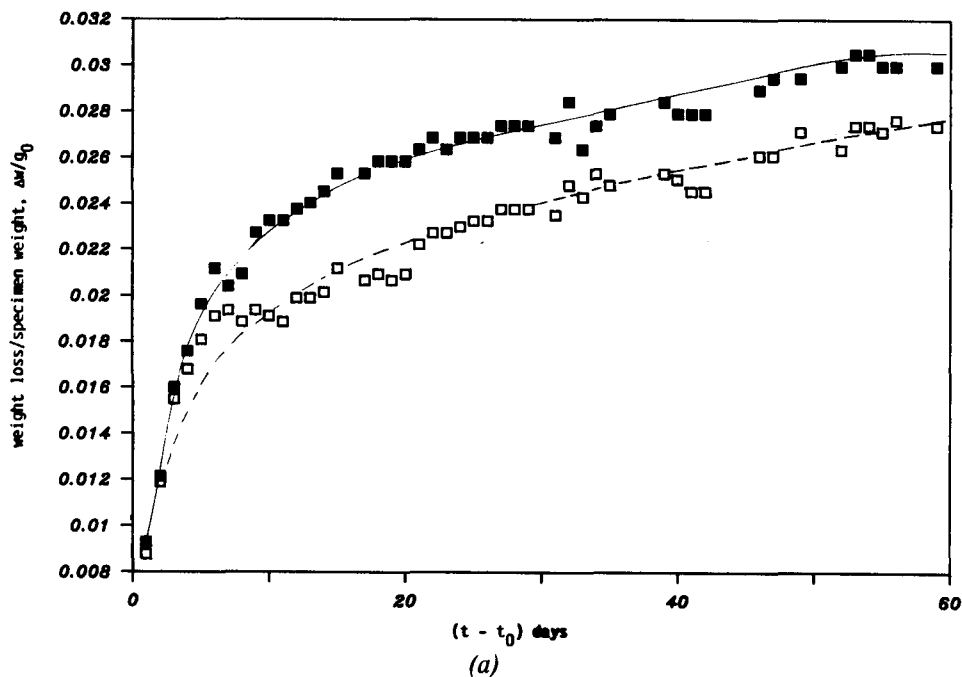


Fig. 5(a) and (b) — Measured relative weight loss of two specimens with No. 3 bars.

uncracked concrete — the two contributions being effectively superimposed. This indicates that the rate of drying in the cracked specimens should initially be higher, as is seen on the weight curves.

An attempt for a simplified upper-bound estimate of the contribution of uniformly spaced cracks to the overall drying of cracked concrete in the direction of cracks was made by Bažant and Raftshol.⁵ The authors assumed a viscous laminar flow through the cracks imagined as planar layers of constant thickness δ with spacing s . In their Eq. (39) they found the additional permeability and diffusivity to be proportional to $k_c \delta^3/s$ where $k_c = (\rho_v p_s / 12 \mu_v) \partial h / \partial w$; ρ_v = mass density of water vapor, p_s = saturation vapor pressure for the given temperature, μ_v = viscosity of water vapor, and $\partial h / \partial w$ = slope of the desorption isotherm plotted as

relative humidity h versus specific water content w . Based on this result, the equation for moisture flux J and the diffusion equation of drying of cracked concrete may be written approximately as

$$J = \frac{a}{g} \text{grad } p_v, \quad \frac{\partial h}{\partial t} = C \nabla^2 h \quad (1)$$

in which p_r = vapor pressure and

$$a = \phi a_0, \quad C = \phi C_0 \quad (2)$$

with

$$\phi = 1 + k_c \frac{\delta^3}{s} \quad (3)$$

Here g = gravity acceleration (introduced solely for convenient dimensionality), a = permeability coefficient, C = diffusivity, a_0 and C_0 = their reference values for uncracked concrete, and ϕ = coefficient indicating the ratio of increase of permeability and diffusivity due to cracking.

Since the cracks in reality do not have a constant thickness and smooth planar walls, and the widely open parts of cracks are no doubt discontinuous, the aforementioned theoretical expression for coefficient k_c cannot be used. Coefficient k_c must then be calibrated on the basis of the tests just described. Based on our preceding comments on the differences between the first and second drying periods, only the weight measurements for the first period, during which the weight curves are diverging and are affine to each other, can be used for our purposes. For the sake of simplicity, we will assume that coefficient ϕ has approximately the same value for all points of the specimen during the initial drying period. This could be accurate only at the very beginning of drying, and there is no doubt that appreciable nonuniformities in the distribution of ϕ will develop later. Nevertheless, lacking more sophisticated test results we have to content ourselves with assuming the coefficient ϕ to be approximately uniform and constant throughout the specimen.

Introduce now nondimensional time θ such that $\theta = \phi t$. Then, noting that $\partial/\partial t = \phi \partial/\partial \theta$, the equation $\partial h/\partial t = X \nabla^2 h$ takes the form

$$\frac{\partial h}{\partial \theta} = C_0 \nabla^2 h \quad (4)$$

from which ϕ is absent. Thus, the curves of weight loss should be identical when plotted versus θ rather than t . This indicates that coefficient ϕ may be determined as follows: (1) Plot the curves of specific weight loss Δw (i.e., total weight loss of the specimen divided by specimen volume) versus $\log t$, and determine the mean curves for the specimens with and without cracks [see the solid and dashed curves in Fig. 4(b)]; and (2) Noting that $\log \theta = \log t + \log \phi$, the value of $\log \phi$ represents the mean horizontal distance between these two curves in the initial drying period (i.e., up to about 130 days). The distance $\log \phi$ is marked in Fig. 4(b). In this manner, it is found from Fig. 4(b) that $\phi = 2.34$ for No. 2 bars and 2.16 for No. 3 bars. Since $\delta = 0.10$ mm and $s = 60$ mm on the average, we obtain approximately $k_c \approx 8 \times 10^4 \text{ mm}^{-2}$ for No. 2 bars and $k_c \approx 9.3 \times 10^4 \text{ mm}^{-2}$ for No. 3 bars. In theory these values should be the same, and their difference represents the experimental error. Since the tests and their evaluation is quite crude, we round off the results as

$$k_c = 10^5 \text{ mm}^{-2} \quad (5)$$

This value, along with Eq. (2) and (3), is the principal result of the present study. Along with Eq. (2) and (3) this result can be directly introduced into the existing finite element programs for the calculation of drying of

concrete,¹ including the more realistic programs that treat this problem as nonlinear, with diffusivity depending on pore relative humidity.³

In calculating coefficient k_c , it would of course be better to take into account the fact that the crack width is not really constant. Moreover, drying might cause the width of the cracks initially created by bending to increase slightly even though the tie rod prevents a significant crack width increase, as confirmed by the present observations of crack width. The crack width increase due to drying must be smaller in the interior of the specimen than at the crack mouth where the crack width is observed by microscope. Due to lack of data, we ignore these effects although this simplification is probably not too serious.

Although we call the companion specimens "uncracked," we should keep in mind that they no doubt contain densely distributed invisible microcracks due to the nonuniformity of shrinkage. These microcracks, which could be eliminated only by superimposed triaxial compression, probably have a negligible influence on drying.

PHYSICAL HYPOTHESIS

Appreciable though the effect of cracking is according to present test results, it is nevertheless far smaller than the bound calculated under the assumption that the cracks are of constant thickness, have planar walls, and are continuous. Under that assumption, it was shown by Bažant and Raftshol⁵ that cracks of widths 0.3 mm and spacing $s = 300$ mm would increase the overall drying permeability and diffusivity of concrete in the direction of the cracks about 1000 times. This would mean that planar cracks of a constant 0.3 mm width and spacing $s = 70$ mm should increase the drying permeability or diffusivity about 4290 times. Thus, the cracks as presently observed ($\delta = 0.1$ mm and $s = 70$ mm) should increase it about 160 times. This bound is two orders of magnitude larger than the present experimental results.

Obviously, as suspected by Bažant and Raftshol,⁵ this comparison implies that the major cracks must be discontinuous even though they are seen to be continuous on the surface. This leads us to advance the following hypothesis: The crack passages for water in the invisible interior of the specimen may have very narrow necks.

The situation may be idealized as shown in Fig. 6, in which δ = width of the major cracks, $\alpha\delta$ = width of the necks ($\alpha < 1$), l = spacing of the necks, βl = length of the necks ($\beta < 1$), and s = spacing of the major cracks. If $\alpha \ll 1$, the resistance of the wide-crack segments of length $(1 - \beta)l$ to the flow of water is negligible compared to the resistance of the necks. The reason is that the resistance to flow is generally proportional to the cube of pore width if the flow is laminar (viscous) rather than turbulent. Therefore, one may assume that permeability is controlled solely by the necks. This means that δ in Eq. (3) should be replaced by $\alpha\delta$. Furthermore, the permeability should decrease in pro-

portion to the length fraction β occupied by the necks (Fig. 6). So, in analogy to Eq. (3), we have

$$\phi = 1 + \frac{k_0 (\alpha\delta)^3}{\beta s} \quad (6)$$

in which k_0 is a coefficient characterizing crack passages with necks. By comparison with Eq. (3)

$$k_c = \frac{\alpha^3}{\beta} k_0 \quad (7)$$

The necks considered alone can now be treated as pores of constant width with planar walls. Therefore, the aforementioned calculation results based on Eq. (39) of Bažant and Raftshol⁵ should really be applied to the necks rather than the cracks as a whole. Thus, the predicted 160-fold increase of permeability means that $1 + k_0 \delta^3/s = 160$. Assuming that $\beta = 0.1$, Eq. (6) then yields our measured value $\phi = 2.25$ if we assume that $\alpha = [1.25 \times 0.1/(160 - 1)]^{1/3} \approx 0.1$. For $\beta = 0.3$ this result would change to $\alpha = 0.13$, and for $\beta = 0.03$, it would change to $\alpha = 0.06$, which shows that the value of α is not too sensitive to the assumed value of β .

So we see that our measurements can be explained by the hypothesis that the cracks in the interior of the specimen differ from those visible at the surface by the presence of necks that are about 10 times narrower than the major cracks. This hypothesis does not seem unreasonable if we realize that the surface layer of concrete differs in its properties from the interior concrete. This is called the wall effect² and is due to the fact that the surface layer always contains a smaller fraction of aggregate and a larger fraction of cement mortar. The mortar is normally softer and, due to its higher homogeneity, cracks should localize in the surface layer more easily than they can in the specimen interior. It might be that a similar effect plays some role in fracture mechanics, causing the cracking in the fracture process zone in the specimen interior to be more discontinuous, and thus less localized than visible at specimen surface.

It may be also noted that a similar hypothesis about necks on the water passages in concrete was used earlier⁷ to explain the discovery made at Northwestern University that the permeability increases by about two orders of magnitude if concrete is heated above 100 C.

CONCLUSIONS

1. A C-shaped beam with a tie rod, reinforced on the tensile face, represents a suitable specimen for studying the effect of crack width upon drying permeability and diffusivity of cracked concrete.

2. Cracks of width 0.1 mm have an appreciable effect on the overall rate of drying (moisture diffusion) of cracked concrete in the direction of cracking. When spaced at 70 mm, they increase the drying permeability and diffusivity by about 2.25 times.

3. Based on a simplified theory, the additional permeability and diffusivity due to cracking is propor-

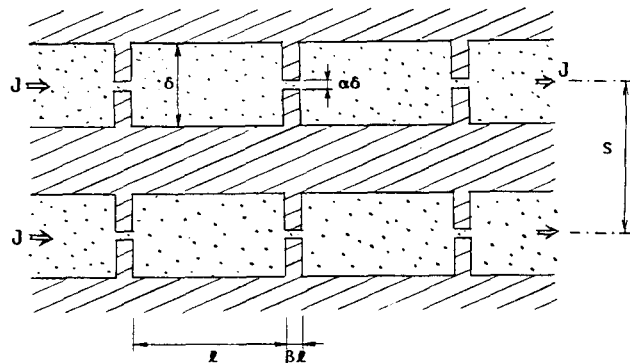


Fig. 6 — Idealized shape of major cracks

tional to the crack width cubed and inversely proportional to the crack spacing.

4. The permeability and diffusivity increase due to cracking is about two orders of magnitude less than predicted on the basis of the hypothesis stating that the cracks are of constant thickness, have planar walls, and are continuous.

5. The measured results, however, can be explained by Bažant and Raftshol's⁵ formula based on water vapor viscosity if it is assumed that the major cracks in the specimen interior, unlike those visible on the surface, are discontinuous, being interrupted by necks that are about 10 times narrower than the major cracks produced by loading.

ACKNOWLEDGMENTS

Thanks are due to the U. S. National Science Foundation for partial financial support under Grant No. FED-7400 (Program Director Dr. Gifford H. Albright) to Northwestern University. Jin-Keun Kim as graduate research assistant and Siddik Şener as visiting scholar participated in the present project at Northwestern University in its first and second stages, respectively.

REFERENCES

1. RILEM Committee TC69, "State-of-the-Art Report on Creep and Shrinkage of Concrete: Mathematical Modeling," *Preprints*, 4th RILEM International Symposium on Creep and Shrinkage of Concrete: Mathematical Modeling, Northwestern University, Evanston, Aug. 1986, pp. 39-455.
2. Neville, Adam M., *Properties of Concrete*, 3rd Edition, Pitman Publishing Co., London, 1981, 779 pp.
3. Bažant, Z. P., and Najjar, L. J., "Nonlinear Water Diffusion in Nonsaturated Concrete," *Materials and Structures, Research and Testing* (RILEM, Paris), V. 5, No. 25, Jan.-Feb. 1972, pp. 3-20.
4. Jonasson, J.-E., "Slipform Construction—Calculations for Assessing Protection Against Early Freezing," *Forskning/Research* No. 4:84, Swedish Cement and Concrete Research Institute, Stockholm, 1984, 70 pp.
5. Bažant, Zdeněk P., and Raftshol, Warren J., "Effect of Cracking in Drying and Shrinkage Specimens," *Cement and Concrete Research*, V. 12, No. 2, Mar. 1982, pp. 209-226.
6. Bažant, Z. P.; Şener, S.; and Kim, J.-K., "Effect of Cracking on Moisture Diffusion through Concrete and Shrinkage," *Preprints*, 4th RILEM International Symposium on Creep and Shrinkage of Concrete: Mathematical Modeling, Northwestern University, Evanston, Aug. 1986, pp. 879-884.
7. Bažant, Zdeněk P., and Thonguthai, Werapol, "Pore Pressure and Drying of Concrete at High Temperature," *Proceedings*, ASCE, V. 104, EM5, Oct. 1978, pp. 1059-1079.